NEW DATA ON POLYMORPHS OF ANHYDROUS DICALCIUM ORTHOSILICATE

Natalia A. Yamnova, Yuriy K. Egorov-Tismenko, Elena R. Gobechiya
Faculty of Geology, Moscow State University, Moscow, natalia-yamnova@yandex.ru

Alexander E. Zadov
OOO «NPP TEPLOHIM», Moscow, AEZadov@yandex.ru

Victor M. Gazeev
Institute of Geology of Ore Deposits, Petrography, Mineralogy and Geochemistry, RAS, Moscow

This article describes new data on polymorphous modifications (α, α'_L, α'_H, β, γ) of Ca_2SiO_4. Structural features and mechanisms of phase transition between Ca_2SiO_4 polymorphs interrelated to modifications of K-Na sulfate aphthitalite (glaserite) $K_3Na[SO_4]_2$ have been analyzed with regard to modular theory and theory of the closest packing. The major structural module $^{[12]}M(1)^{[6]}M(1')^{[10]}M(2)_2[TO_4]_2$ (M = K, Na, Ca, Mg; T = S, Si) has been revealed for the Ca_2SiO_4 modifications and relative natural "glaserite-type" silicate minerals, bredigite $Ca_7Mg[SiO_4]_4$ and merwinite $Ca_3Mg[SiO_4]_2$; and calcio-olivine (γ-Ca_2SiO_4) examined by the authors. The structural glaserite modules similar in symmetry and composition in the structures of described compounds account for topotactic character and reversible phase transition between the Ca_2SiO_4 polymorphs on the one hand and abundant assemblages of the mineral series on the other.

5 tables, 15 figures, 26 references.

Keywords: calcium orthosilicate, new mineral, polymorphous modifications, phase transfictions.

Calcio-olivine (γ-Ca_2SiO_4)[1] (Zadov *et al.*, 2008; Gobechiya *et al.*, 2008) pertains to a series of polymorphous modifications of Ca_2SiO_4 (α, α'_L, α'_H, β, γ), based on the running order of decreasing temperature at which these phases are stable (Taylor, 1996):

$$\alpha \underset{1425^\circ C}{\rightleftarrows} \alpha'_H \underset{1160^\circ C}{\rightleftarrows} \alpha'_L \underset{630-680^\circ C}{\rightleftarrows} \beta \underset{< 500^\circ C}{\rightarrow} \gamma$$

$$\uparrow_{780-860^\circ C} \quad \downarrow_{690^\circ C}$$

The first four modifications are close to the structural type of K-Na sulfate aphthitalite (glaserite) $K_3Na[SO_4]_2$ that causes reversible transitions between them. High-temperature and low-temperature modifications related by phase transitions are known among the "glaserite-type" sulfates. Belonging to the same structural type suggests similar structural transformations between aphthitalite (glaserite) polymorphs on the one hand and dicalcium orthosilicate on the other. However, in studies concerned with crystal chemistry of the Ca_2SiO_4 polymorphs (Eysel and Hahn, 1970; Barbier and Hyde, 1985; Il'inets and Bikbau, 1990), such comparison is absent, despite reference of their affinity to the glaserite structural type. In addition, these studies are based on ambiguous investigation results of single crystals of solid solutions $Ca_2SiO_4-Ca_2GeO_4$, $Ca_2SiO_4-Sr_2SiO_4$, $Ca_2SiO_4-Ba_2SiO_4$, which are structural analogues of high-temperature Ca_2SiO_4 modifications and contain Sr and Ba admixtures used as stabilizers (along with additives V_2O_5, Al_2O_3, Cr_2O_3, and $Na_2P_4O_7$) to synthesize qualitative single crystals.

In this study, we examined features of structure and mechanisms of phase transitions between the Ca_2SiO_4 polymorphs interrelated with modifications of aphthitalite (glaserite) using results of structure refinement of pure calcium compounds by Rietveld method on the basis of X-ray powder diffraction: at high temperature using neutron radiation (Mumme *et al.*, 1996) and under ambient conditions using X-ray radiation (Gobechiya *et al.*, 2008). The review has been supplemented with comparison of the structures of bredigite $Ca_7Mg[SiO_4]_4$ and merwinite $Ca_3Mg[SiO_4]_2$, which are natural glaserite-type silicate minerals similar to synthetic modifications of dicalcium orthosilicate (Table 1).

This is the last crystal chemical review prepared with participation by Yuriy K.

[1] The mineral species was approved by the Commission on New Minerals, Nomenclature and Classification of the International Mineralogical Association in September 06, 2007.

Table 1. **Crystallography of some natural and synthetic glaserite-type compounds**

Compound, formula	Unit-cell dimensions (Å, degree) *a* *b* *c* α β γ	Space group	*Z*	*V*(Å^3)	ρ_{calc} (g/cm^3)	Source
Aphthitalite (glaserite) $K_3Na[SO_4]_2$	5.680 7.309	$P\bar{3}m1$	1	204.2	2.66	Okada & Ossaka, 1980
α-K_2SO_4 (700°C)	5.947 8.375	$P6_3/mmc$	2	433.9	2.63	Miyake *et al.*, 1980
Arkanite β-K_2SO_4	7.476 5.763 10.071	*Pnma*	4	194.2	2.91	McGinnety, 1972
α-Ca_2SiO_4 (1545°C)	5.532 7.327	$P6_3/mmc$	2	256.5	2.23	Mumme *et al.*, 1996
		$P\bar{3}m1$	2			
α'_H-Ca_2SiO_4 (1250°C)	6.871 5.601 9.556	*Pnma*	4	367.8	3.07	Mumme *et al.*, 1996
α'_L-Ca_2SiO_4 (1060°C)	20.527 5.590 9.496	$Pn2_1a$	12	1089.6	3.11	Mumme *et al.*, 1996
Larnite β-Ca_2SiO_4 (630−680°C)	6.745 5.502 9.297 94.59	$P2_1/n11$	4	343.9	3.28	Jost *et al.*, 1977
Calcio-olivine γ-Ca_2SiO_4	5.074 6.754 11.211	*Pcmn*	4	384.2	2.94	Gobechia *et al.*, 2008
Merwinite $Ca_3Mg[SiO_4]_2$	13.254 5.293 9.328 91.90	$P12_1/a1$	4	1348.3	3.27	Moore & Araki, 1973
Bredigite $Ca_7Mg[SiO_4]_4$	6.739 10.909 18.340	*Pn2n*	2	654.0	3.29	Moore & Araki, 1976

Notes: Orthorhombic and monoclinic compounds are in settings suitable for comparison.
Temperatures at which phases are stable are in parentheses.

Egorov-Tismenko (1938−2007), associate professor, Division of Crystallography, Faculty of Geology, Lomonosov Moscow State University, famous teacher and scientist, who made significant contribution to crystallography, crystal chemistry, and structural mineralogy. This article is dedicated to his memory.

Aphthitalite (glaserite) and its polymorphs

Numerous natural and synthetic sulfates, phosphates, silicates, germanates, arsenates, and other compounds whose structures are characterized by certain atom arrangement are attributed to the structural type of aphthitalite (glaserite) $K_3Na[SO_4]_2$. In space group $P\bar{3}m1$, large cations Na^+, K^+, Ca^{2+}, Sr^{2+}, and Ba^{2+} occupy regular point systems of symmetry $\bar{3}m$ in sites *M*(1) and *M*(1′) with coordinates (0, 0, 0); (0, 0, 1/2) and on the 3-fold axes in site *M*(2) (1/3, 2/3, *z*), where central cations (S^{4+}, Si^{4+}, P^{5+}, Ge^{4+}) and apical O-vertices of tetrahedra are also arranged. Oxygen vertices of tetrahedron triangular bases are localized in symmetry plane *m* with coordinates (*x*, −*x*, *z*).

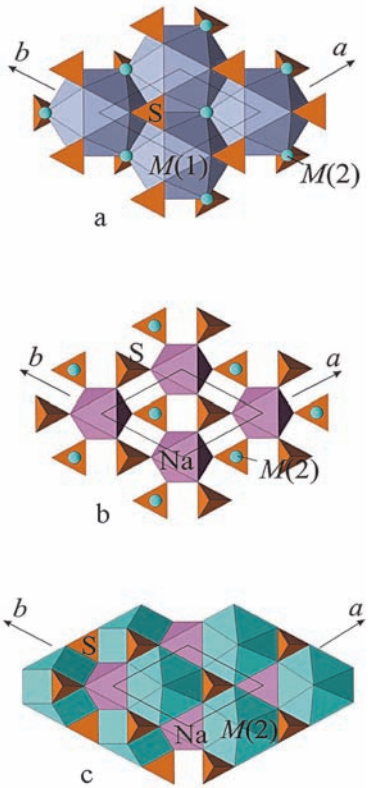

Fig. 1. Fragments (sheets) of the structure of aphthitalite (glaserite) projected onto (0001). (a) Sheet consisting of M(1) icosahedra and SiO_4 tetrahedra; (b) linkage of M(1′) octahedra and SO_4 tetrahedra; (c) sheet consisting of the M(2) 10-fold polyhedra, SO_4 tetrahedra, and M(1′) octahedra.

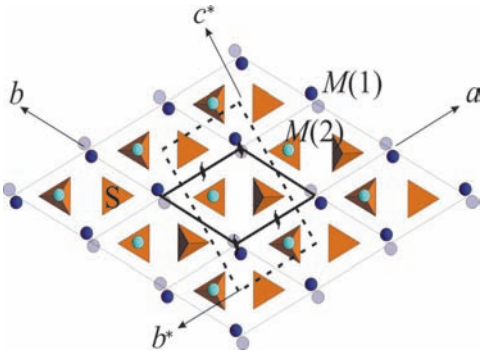

Fig. 2. Relationship of the unit cells of aphthitalite (glaserite) $K_3Na[SO_4]_2$ (solid thick line) and arkanite β-K_2SO_4 (dashed line).

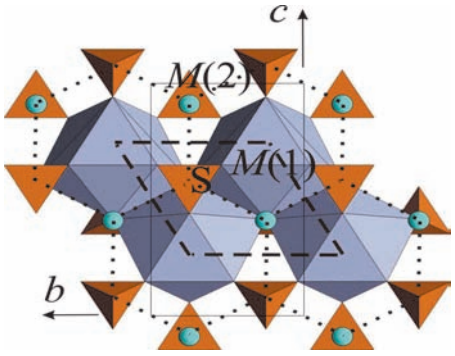

Fig. 3. Zigzag ribbons composed of M(1) 9-fold polyhedra projected onto (100) of the structure of arkanite β-K_2SO_4. Icosahedra of the primary structure of glaserite are delineated by dotted line and its unit cell, by dashed line. Solid line delineates the unit cell of arkanite.

The structure of aphthitalite (glaserite) $K_3Na[SO_4]_2$ (Bellanca, 1943; Moore, 1976; Okada and Ossaka, 1980) is sufficiently close framework consisted of large K polyhedra and Na octahedra with isolated $[SO_4]$ tetrahedra in cavities. Two types of sheets parallel to (0001) can be recognized in the framework. The first one (-0.2 to $+0.2$ thick along z) is composed of edge-sharing distorted centrosymmetrical K icosahedra with centres in sites $M(1)$ bonded by shared horizontal edges. Six $[SO_4]$ tetrahedra surrounding $M(1)$ icosahedron, with each of three vertical edges being shared with neighboring $M(1)$ polyhedron and apical vertex being shared of three $M(1)$ polyhedra of the sheet are attributed to the same layer (Fig. 1a). Six oxygen atoms at distance of 2.909 Å arranged in vertices of two opposite triangular icosahedron faces perpendicular to the 3-fold axis and forming octahedron elongated along axis c compose the first coordination sphere. The second sphere consists of six apical vertices of S tetrahedra arranged in equatorial plane of icosahedron at distance of 3.288 Å. Another more voluminous sheet ($0.2-0.8$ thick along z) is composed of Na octahedra (Fig. 1b) with centres in sites $M(1')$ shared triangular faces with the $M(1)$ icosahedra and face-sharing K 10-fold polyhedra with centres in sites $M(2)$ (Fig. 1c). Each of two $M(2)$ polyhedra of unit cell bonded by inversion centres is half of Archimedean cuboctahedron covered by hexagonal pyramid instead of the second half. Six of ten ligands around the $M(2)$ atom are located in plane (0001) at distance of 2.854 Å; three ligands composing shared face with $[SO_4]$ tetrahedron are distant of 3.112 Å; the tenth ligand opposite to this face being apex of hexagonal pyramid is located 2.547 Å of central atom. This $O(1)$ atom located in equatorial plane of $M(1)$ icosahedron is apical vertex of tetrahedron translational along axis c and located Thus, the second more voluminous sheet of the structure of glaserite consists of $M(1')$ octahedra and $M(2)$ 10-fold polyhedra with vertices of hexagonal pyramids embedded in upper and lower icosahedral sheets. The central Na octahedron called by Moore (1973) as rotator combined with surrounding $[SO_4]$ tetrahedra is the major element of the structures similar to glaserite (Fig. 1b). The lower three tetrahedra ($z \sim 0.2$) of the rotator are shared with the upper three tetrahedra of the first icosahedral layer and upper three tetrahedra ($z \sim 0.8$) of rotator are shared with three tetrahedra of translationally identical sheet along axis c.

Two modifications of K sulfate, low-temperature β-K_2SO_4 (analogue of arkanite) (McGinnety, 1972) and high-temperature synthetic α-K_2SO_4 (Miyake *et al.*, 1980) are assigned to the aphthitalite (glaserite) structural type. Egorov-Tismenko *et al.* (1984) showed that the structure of β-K_2SO_4 can be obtained by rotation of the initial glaserite unit cell (Fig. 2) around axis 2_1 input instead of axis 3 into coordinate origin. Such trans-

formation results in disappearing translations along horizontal axis and appearance of a new vector, which is equal to long diagonal of the glaserite unit cell and perpendicular to preserved translational vector of glaserite along axis *x*. Transition matrix from the glaserite to arkanite unit cell is (001/ $\bar{1}$00/120). In addition, instead of horizontal 2-fold axes and inversion centres located on the (01 $\bar{1}$0) faces of the glaserite unit cell, apothemal planes *c* appear as a result of interaction of input axes $2_1(z)$ with preserved mirror symmetry planes *m* of the glaserite space group $P\bar{3}m1$ perpendicular to axis *b* of the β-K_2SO_4 unit cell. In the new orthorhombic unit cell, slip vector of plane *c* is directed along coordinate *x* that changes the name of this plane to *a*. Residual half of inversion centres of the glaserite space group preserves in orthorhombic space group *Pnma* of β-K_2SO_4 and their interaction with input axes 2_1 accounts for appearance of perpendicular clinoplane *n* localized between inversion centres along vertical axis *a* of the new cell. In the structure of β-K_2SO_4 within the selected glaserite cell, atoms are arranged similarly to those in the glaserite structure. In duplicate orthorhombic cell, O atoms occupy three regular point systems in contrast to two systems in the glaserite structure. Two varieties of O atoms located on planes $m_{\perp y}$ have two degrees of freedom that allows their displacement from the glaserite sites resulting in liquidation of the 3-fold axes. In addition, reflection of the glaserite cell in apothemal plane *c* displaces oxygen atoms O(1), which are apical vertices of S tetrahedra arranged in equatorial plane of *M*(1) icosahedron, to 1/2 *Ta* (coordinate *x* of the β-K_2SO_4 structure). It is reflected in the shape of coordination polyhedra around *M*(1) and *M*(1′) cations. Three of six oxygen atoms of the hexagonal section of *M*(1) icosahedra (12 − 3 = 9) transit to coordination sphere of *M*(1′) cations (6 + 3 = 9) forming the identical polyhedra bonded by screw 2-fold axis (2_1) on two levels on axis *a*. In this case, continuous the *M*(1) icosahedral sheets and *M*(1′) octaredra of the other layer are transformed in the structure of β-modifications into zigzag ribbons consisting of *M*(1) and *M*(1′) 9-fold polyhedra (Fig. 3) elongated along axis *b* of orthorhombic cell and arranged on two levels on axis *a*. As a result, less close framework composed of *M*(1) 9-fold polyhedra, *M*(2) polyhedra, and [SO_4] tetrahedra is formed. Coordination of *M*(2) atoms is unchangeable; only orientation of hexagonal pyramids of *M*(2) 10-fold polyhedra changes. Orientation of part of [SO_4] tetrahedra around *M*(1) polyhedra in the centre of the glaserite rotator also changes (Figs. 4a, 4b).

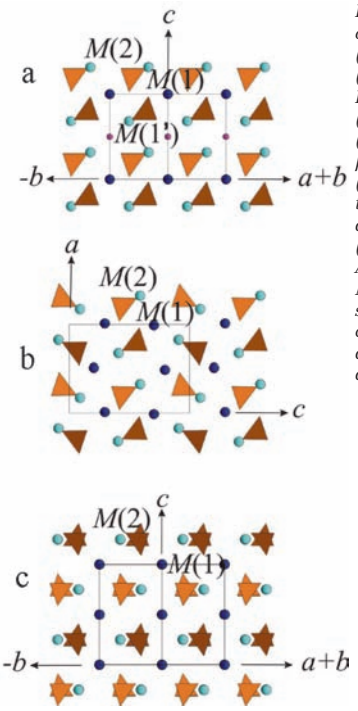

Fig. 4. Projections of the structures: (a) aphthitalite (glaserite) K_3NaSO_4 on (1$\bar{2}$10); (b) arkanie β-K_2SO_4 on (100); (c) high-temperature modification α-K_2SO_4 on (1$\bar{2}$10). Atoms in M(1), M(1′), and M(2) sites are shown by circles. Triangles are tetrahedra around S atoms.

β-K_2SO_4 modification stable within wide range of temperature (from −117^{0}C to 582^{0}C) at 800^{0}C transits to high-temperature α-K_2SO_4 (Miyake *et al.*, 1980), whose symmetry increases up to space group $P6_3/mmc$ in comparison with the initial glaserite symmetry. In the structure of α-K_2SO_4 (Fig. 4c), K_1 atoms occupy regular point system of symmetry $\bar{3}m$ (coordinates 0,0,0 and 0,0,1/2) and K_2 and S atoms occupy system of symmetry $\bar{6}m2$ (coordinates 2/3, 1/3, 1/4 и 2/3, 1/3, and 3/4, respectively). Two alternative mirror-symmetrical tetrahedra with opposite oriented apical vertices and statistically filled sites 4*f* (regular point system of symmetry 3*m* and coordinates 1/3, 2/3, z) and sites 12*k* (symmetry *m* and coordinates *x*, 2*x*, *z*) by O(1) atoms (apical vertices of tetrahedra) and O(2) atoms (vertices of tetrahedron bases), respec-

Table 2. **Distances (Å) cation-anion in coordination polyhedra around sites *M*(1) of the glaserite-type compounds**

Compound, formula	*M*(1)-polyhedron Minimum	Maximum	Average	*M*(1')-octahedron Minimum	Maximum	Average
Aphthitalite (glaserite)	2.91	3.29	[12]3.10	2.39	2.39	2.39
$K_3Na[SO_4]_2$	2.91	2.91	[6] 2.91			
Arkanite β-K_2SO_4	2.73	3.13	[9]2.86	–	–	–
	2.73	2.80	[6] 2.77			
α-K_2SO_4	2.69	3.52	[12]3.28	–	–	–
	2.69	3.41	[6] 3.05			
α-Ca_2SiO_4	2.60	3.53	[12]2.97	2.26	2.26	2.26
space group $P\bar{3}m1$	2.72	2.72	[6] 2.72			
α-Ca_2SiO_4	2.23	3.54	[12]3.08	–	–	–
space group $P6_3/mmc$	2.23	2.75	[6] 2.49			
α'_H-Ca_2SiO_4	2.26	2.85	[8] 2.56	–	–	–
	2.26	2.68	[6] 2.53			
α'_L-Ca_2SiO_4	2.39	2.75	[8]2.58	–	–	–
	2.39	2.71	[6]2.52			
Larnite β-Ca_2SiO_4	2.38	2.64	[8]2.49	–	–	–
	2.38	2.64	[6]2.48			
Calcio-olivine γ-Ca_2SiO_4	2.32	2.47	[6]2.41	–	–	–
Merwinite $Ca_3Mg[SiO_4]_2$	2.31	2.84	[8]2.55	1.99	2.16	2.06
Bredigite $Ca_7Mg[SiO_4]_4$	2.39	3.01	[10]2.79	2.01	2.22	2.11
	2.28	3.28	[10]2.78	2.00	2.12	2.07
	2.31	2.65	[9]2.60			
	2.31	2.72	[8]2.47			

Notes: Average cation-anion distances of two domains are given for α'_H polymorph and three subcells, for a'_L polymoph. Cation-anion distances for independent sites are given for the structures of merwinite and bredigite.

Fig. 5. The structure of α'_H-Ca_2SiO_4 projected on plane (100) (b) and its left (a) and right (c) mirror-symmetrical domains. Ca atoms in M(1) site at levels x ~ 0 (light circles) and x ~ 0.5 (dark circles).

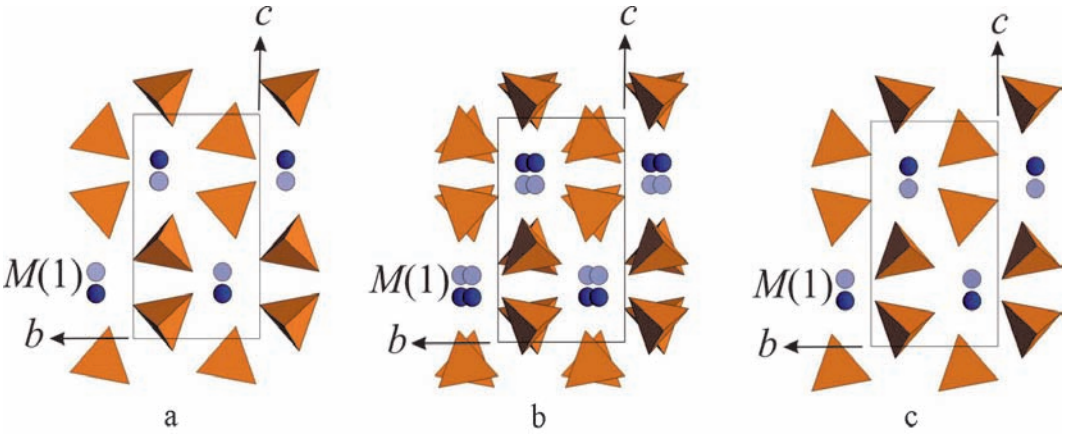

Table 3. **Cation-anion distances (Å) in coordination polyhedra around sites *M(2)* and *T* in the structures of glaserite-type compounds**

Compound, formula	*M*(2)-polyhedron Minimum	Maximum	Average	*T*-tetrahedron Minimum	Maximum	Average
Aphthitalite (glaserite)						
$K_3Na[SO_4]_2$	2.55	3.11	[10]2.90	1.47	1.48	1.47
Arkanite β-K_2SO_4	2.72	3.19	[10]3.00	1.46	1.47	1.47
α-K_2SO_4	2.85	3.87	[10]3.28	1.34	1.35	1.35
α-Ca_2SiO_4	2.06	3.66	[10]2.97	1.58	1.67	1.61
space group $P\bar{3}m1$						
α-Ca_2SiO_4	2.12	3.36	[10]3.03	1.57	1.64	1.58
space group $P6_3/mmc$						
α'_H-Ca_2SiO_4	2.29	3.32	[10] 2.82	1.59	1.65	1.63
α'_L-Ca_2SiO_4	2.32	3.36	[10]2.82	1.53	1.67	1.61
Larnite β-Ca_2SiO_4	2.22	2.88	[7]2.51	1.61	1.65	1.63
Calcio-olivine	2.29	2.39	[6]2.35	1.58	1.69	1.62
γ-Ca_2SiO_4						
Merwinite	2.22	2.81	[9]2.58	1.60	1.66	1.63
$Ca_3Mg[SiO_4]_2$	2.25	3.10	[9]2.64	1.60	1.64	1.62
Bredigite						
$Ca_7Mg[SiO_4]_4$	2.31	3.11	[10]2.67	1.58	1.65	1.61
	2.24		[10]2.69	1.58	1.61	1.61
	2.33	3.15	[10]2.72	1.58	1.66	1.61
	2.33	3.43	[10]2.81	1.60	1.65	1.62

Notes: Average cation-anion distances of two domains are given for α'_H-polymorph and three subcells, for α'_L polymoph. Cation-anion distances for independent sites are given for the structures of merwinite and bredigite.

tively, are formed around sulfur atoms. Two bipolar statistically filled 10-fold polyhedra are formed around K_2 atoms that causes an appearance of horizontal plane m_z and increasing symmetry to holohedral. Coexistence of alternative mirror-symmetrical tetrahedra in the structure of α-modification provides orthogonal unit cell in it, where the structure of β-modification of K_2SO_4 is described (Fig. 4b) accounting for topotactic character of β-K_2SO_4 — α-K_2SO_4 transition previously reported in (Miyake *et al.*, 1980). As seen from Tables 2 and 3, this transition is accompanied with increase of average cation-anion distances in coordination polyhedra around large cations at simultaneous their decrease in S tetrahedra.

High–temperature polymorphs of Ca_2SiO_4

The structures of high-temperature polymorphs of Ca_2SiO_4 are similar to the structures of above glaserite modifications, where the glaserite sites of K and S are replaced by Ca and Si. According to Mumme *et al.* (1996), the structure of α-modification of Ca_2SiO_4 is close to that of high-temperature α-K_2SO_4 (Fig. 4c) but differs from it in greater number of statistically filled atomic sites. In addition to the formation of alternative tetrahedral and 9-fold polyhedra, the displacement of apical O(1) vertices (site 4*f*) of Si tetrahedra from 3-fold axes to form alternative and arranged in one plane sites (12*k*) is observed in the structure of α-Ca_2SiO_4. This results in wide range of Ca-O distances (Tables 2, 3) and strong distorted Ca polyhedra. Mumme *et al.* (1996) reported in the examined sample the second component, whose structure is described in the frame of the glaserite model (space group $P\bar{3}m1$) differed from the latter in analogous displacement of O(1) atoms from 3-fold axis.

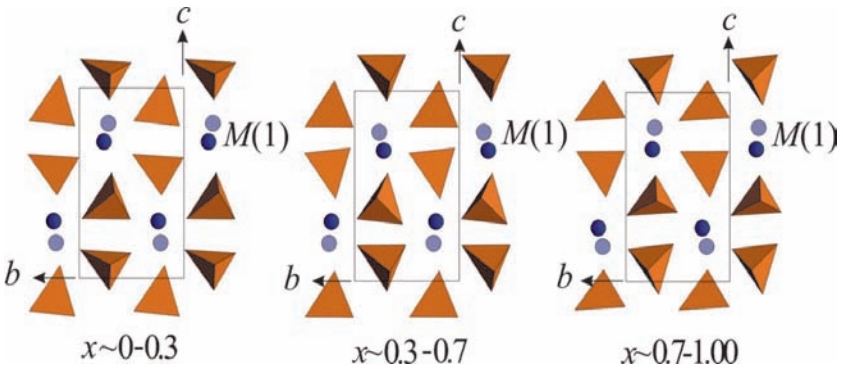

Fig. 6. The structure of α'_L-Ca_2SiO_4 projected onto (100). Subcells at three levels on axis x are shown. Light and dark circles are Ca atoms in sites M(1) with x ~ 0.17.

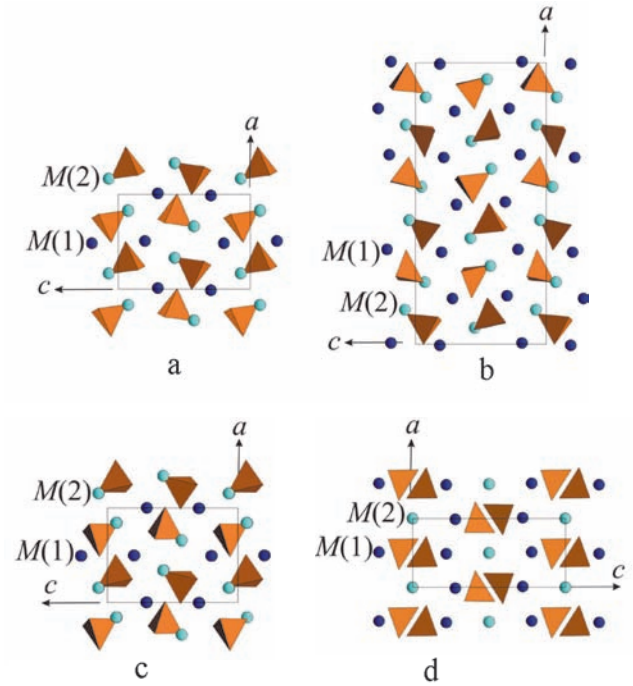

Fig. 7. The structures of polymorphs of dicalcium orthosilicate onto (010): (a) α'_H-Ca_2SiO_4; (b) α'_L-Ca_2SiO_4; (c) β-Ca_2SiO_4; (d) γ-Ca_2SiO_4.

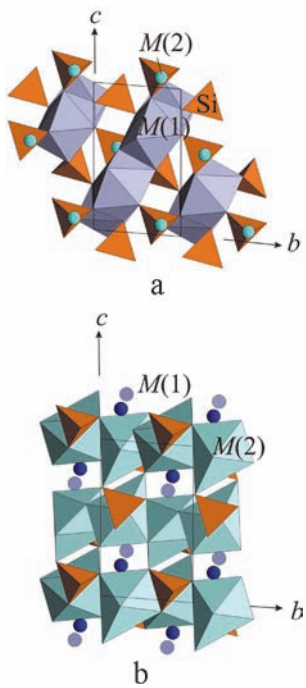

Fig. 8. The structure of β-Ca_2SiO_4 projected on plane (100): (a) sheets consisting of M(1) 8-fold polyhedra; (b) framework composed of M(2) 7-fold polyhedra. Ca atoms in site M(1) at levels x ~ 0 (light circles) and x ~ 0.5 (dark circles).

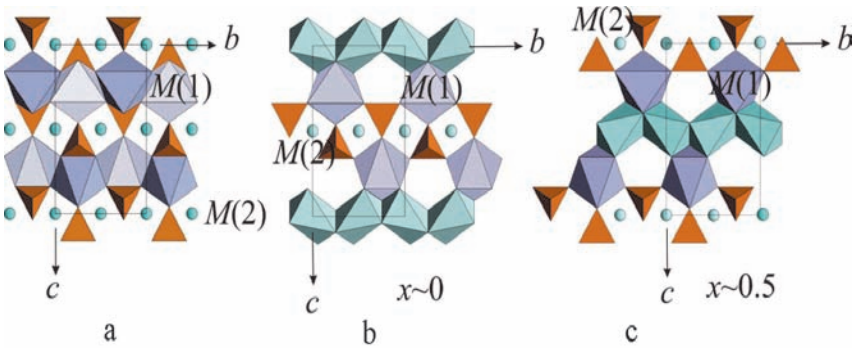

Fig. 9. Fragments of the structure of calcio-olivine γ-Ca_2SiO_4 projected onto (100): (a) wall composed of the M(1) octahedra; (b, c) olivine ribbons consisting of the M(2) octahedra with toothing of the M(1) octahedra at levels x ~ 0 and x ~ 0.5, respectively.

In the structures of orthorhombic α'_H- and α'_L modifications of Ca_2SiO_4 (Table 1), the model of the β-K_2SO_4 structure is repeated but it is distorted due to atomic atoms displaced from corresponding sites. In the structure of α'_H-Ca_2SiO_4 (Figs. 5a, 5b, 5c, 7a) this leads to the formation of two mirror-symmetrical ($m_{\perp b}$) domains (space group $Pn2_1a$) with statistically filled all sites (with the exception of Si) and in the structure of α'_L-Ca_2SiO_4, to threefold one of the unit-cell dimensions (6.84 x 3 = 20.53 Å). In the last case, in addition to displaced O and Ca atoms, turn of Si tetrahedra and their distortion are observed in subcells neighboring on axis *a* (Figs. 6a, 6b, 6c, 7b). Distinctions of hexagonal α- and ortjorhombic α'_H- и α'_L- modifications of Ca_2SiO_4 are similar to those described for glaserite and concern with modified orientation of tetrahedra in the glaserite rotator resulting in decreasing number of ligands around Ca in *M*(1) site. In addition to these distinctions, in the structures of α'_H- and α'_L-modifications, atomic displacement results in distance one of three equatorial vertices of *M*(1) 9-fold polyhedra from central Ca (3.20 Å in α'_H-Ca_2SiO_4; and 3.39, 3.43, and 3.56 Å in three neighboring subcells in α'_L-Ca_2SiO_4, respectively) and their conversion into 8-fold polyhedra (Table 2), which are edge-shared only with two Si tetrahedra. *M*(1) 8-fold polyhedra form framework consisting of zigzag columns elongated along axis *a* of unit cell, rather than bands in the structure of β-K_2SO_4. Each of these columns is formed by edge-sharing polyhedra along [100] and [001], and vertex-sharing, along [010]; the latter is true for the averaged α'_H-Ca_2SiO_4 model. Polyhedra around Ca in *M*(2) site are close in shape to corresponding polyhedra in the structure of α-Ca_2SiO_4 (for model with pace group $P\bar{3}m_1$) and characterized by the greater distortion degree (Table 3). The Si-O distances in the structure of α'_H-modifications are within usual range, whereas, in the structure of α'_L-modification, their small deviation is observed (Table 3).

Low-temperature polymorphs of Ca_2SiO_4

Synthetic analogue of larnite β-Ca_2SiO_4 is metastable phase that at temperature below 500°C transits into γ-modification (Figs. 7c, 7d). The structure of β-Ca_2SiO_4 was examined for the first time by Midgley (1952) on the basis of crystals stabilized by 0.5% B_2O_3. Later, the structure was refined using pure Ca (Jost *et al.*, 1977) and Sr (Catti *et al.*, 1983) crystals synthesized without stabilizers. Crystals of both compounds were twinned by plane (010) corresponding to the mirror symmetry plane linking two domains in the structure of α'_H-Ca_2SiO_4 at certain arrangement of axes of unit cell (Table 1). The structure of β-Ca_2SiO_4 was also refined by Rietveld method for powder (Mumme *et al.*, 1995). All three models are characterized by the same geometry of atomic arrangement (Fig. 8) and close to the structure of each domain of α'_H-Ca_2SiO_4. Like the structures of orthorhombic polymorphs, Ca atoms in site *M*(1) are surrounded by eight ligands, six of which are located in octahedron vertices and the other two — apical vertices of Si tetrahedra — are arranged in equatorial plane; the third apical vertex is distant from central cation for ~3.5 Å. Atomic displacement in the structure of β-modification results in decrease of the nearest neighbors around Ca in site *M*(2) to 7 (Table 3) and changing way to form polyhedra. Columns consisting of *M*(1) 8-fold polyhedra elongated along axis *a* of unit cell are similar to above described and form sheet parallel to (0 $\bar{1}$1) (Fig. 8a) rather than linked into framework like structures of orthorhombic polymorphs. These sheets are "broached" along axis *b* by zigzag columns consisting of *M*(2) 7-fold polyhedra and linked to each other by shared O vertices into tracery framework (Fig. 8b).

Transition of β-modification to γ-Ca_2SiO_4 is accompanied by substantial transformation of the structure. In the structure of β-Ca_2SiO_4, pairs of Ca atoms in site *M*(1) are bonded by 2-fold screw axes and arrange along axis *a* of unit cell practically each below other (at distance of 3.5 Å, approximately 1/2*Ta*). In the structure of γ-Ca_2SiO_4, these pairs are displaced with regard to each other (distance between them is ~ 4.3 Å) for a half of translation along two axes (*a* and *b*) and centre octahedra linked into tracery walls parallel to (001) (Fig. 9a), where empty and occupied octahedra alternate in staggered rows. In the structure of β-Ca_2SiO_4, Ca atoms in *M*(2) site arranged over and below Si tetrahedra Ca form centrosymmetrical pairs around sites 2*a*

(0,0,0) и 2*d* (1/2,0,1/2). In the structure of γ-Ca_2SiO_4, Ca atoms in sites *M*(2) occupy fixed position in centres of symmetry (site 4*a*, coordinates 0,0,0 и 1/2,0,1/2) and like Ca in site *M*(1) are octahedrally coordinated. Edge-sharing *M*(2) octahedra form olivine-like bands, which are elongated along axis *b* of the unit cell and arranged on two levels on axes *a* and *c* (Fig. 9b, 9c). Change of arrangement of Ca atoms is accompanied with displacement and turn of Si tetrahedra. In the structure of β-Ca_2SiO_4, the *M*(1) central cation of the glaserite rotator is surrounded by six Si tetrahedra, whose centres are located by triplets on two levels (approximately +1/4 and −1/4) on axis *a* with regard to site *M*(1). In the structure of olivine-type γ-Ca_2SiO_4, M(1) octahedron is vertex-shared with five Si tetrahedra, three of which have centres arranged approximately at the same level with site *M*(1) and two are displaced for +1/2*Ta* and −1/2*Ta* with one of which *M*(1) octahedron is edge-sharing and with the other, is vertex-shared. As a result, each Si tetrahedron in the structure of γ-Ca_2SiO_4 shares 3 horizontal edges with two *M*(2) octahedra and *M*(1) octahedron, while vertical edges of Si tetrahedra are free.

Close-packed sheets in the glaserite- and olivine-type structures

In the structure of glaserite, oxygen atoms are not close-packed; however, three types of heterogeneous close-packed sheets composed of O and K atoms parallel to plane (0001) can be recognized. Sheet *I* at level *z* ~0 (Fig. 10a) consists of hexagons of oxygen atoms (apical vertices of tetrahedron) around K atoms in site *M*(1). In ideal closest packing (CP), spheres of the next sheet should be arranged in holes of antecedent one. In the structure of glaserite, distortion of CP is caused by rotation of oxygen triangles around axes 3 by ~30° counterclockwise at level *z* ~ 1/3 (sheet *II*) and clockwise, at level *z* ~ 2/3 (sheet *III*). As a result of such turn, vacancies occupied by K atoms (centres of 10-fold polyhedra in *M*(2) site) arranged over or below oxygen atoms of sheet *I* violating CP of the whole structure are formed in the new sheets. Regard to each other, sheets *II* and *III* are arranged according to principle of CP to form octahedral "cavities" occupied by Na cations (in site M(1′) with coordinates 0,0,1/2). Octahedron elongated along axis *z*, the first coordination sphere around K cation (site *M*(1) with coordinates 0,0,0), is formed between three oxygen atoms of sheet *II* (level *z* ~ 1/3) and sheet *III* arranged at level *z* ~ −1/3, i.e., translational to initial layer. Tetrahedral cavities occupied by S atoms are formed between sheets *I* and *II* and *III* and *I*. In the former case, cavity centres are arranged at *z* ~ 0.2, in the latter, at level *z* ~ 0.8. In doing so, tetrahedra of neighboring levels are opposite oriented along axis *z*. Moore (1976, 1981) noted that turn of oxygen threes of sheets *II* and *III* relative to the first sheet leads to closer occupation of space in comparison with classic homogeneous packing and lesser volume of obtained vacant cavity. In the structure of glaserite, distances between the nearest neighbors in sheets *II* and *III* are 2.85 Å (*M*(2) − O), 2.40 Å (edge of tetrahedron), and 3.28 Å (edge of octahedron) and shorter comparatively to corresponding distances in sheet I, which are 3.29 Å (M(1) − O) and 3.31 Å (O − O). In sheets II and *III*, sum of distances between O atoms corresponding to the edge of octahedron and tetrahedron is the a unit-cell dimension of glaserite (2.40 + 3.28 = 5.68 Å), while sum of octahedron heights around Na (2.92 Å) and K (4.39 Å), dimension *c* (7.31 Å).

In the structure of high-temperature modification α-Ca_2SiO_4, such glaserite heterogeneous close-packed sheets are only characteristic of model with space group $P\bar{3}m1$. Distinction is wider range of distances between neighboring atoms in sheet *I* caused by displacement of O(1) atoms from fixed position on 3-fold axis: 2.60 − 3.53 Å (*M*(1) − O) and 1.03 − 3.54 Å (O − O), herewith, anomalous lower limit of the O − O distance is resulted from statistical occupation of three closely spaced sites by O atoms. In sheets *II* and *III*, interatomic distances are 2.78 Å (*M*(2) − O) and 2.63 − 2.90 Å (O − O). Due to alternative tetrahedra and 10-fold polyhedra, glaserite packing for model of α-Ca_2SiO_4 with space group $P6_3/mmc$ is violated.

In the structure of orthorhombic arkanite β-K_2SO_4 and its Ca-Si analogues, K(Ca) atoms in site *M*(1) and apical oxygen vertices form bands arranged at levels *x* ~ 0 and ~ 1/2

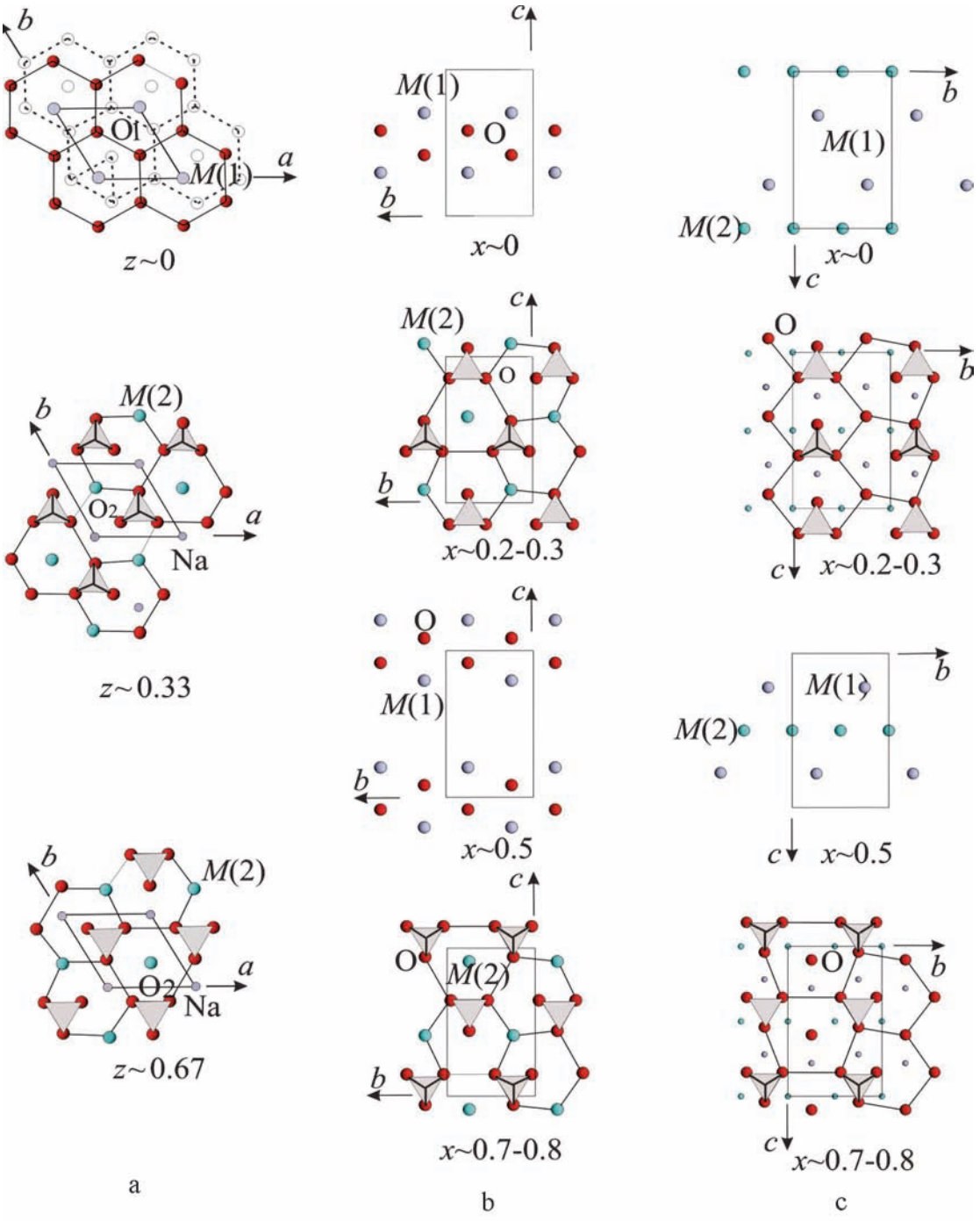

Fig. 10. Close-packed sheets in the structures of: (a) glaserite $K_3Na[SO_4]_2$ (sheets with the ideal closest packing are shown by dashed line); (b) arkanite β-K_2SO_4, rhombic α'_H-, α'_L-, and monoclinic modifications of Ca_2SiO_4; (c) calcio-olivine γ-Ca_2SiO_4. Small circles: centres of octahedral sites.

Table 4. **Valence forces in anions for various structural models of β-Ca_2SiO_4**

O(1) $2M(1)+M(2)+Si$	O(2) $2M(1)+2M(2)+Si$	O(3) $2M(1)+2M(2)+Si$	O(4) $2M(1)+2M(2)+Si$	Source
1.985	1.965	1.944	1.883	Jost *et al.*, 1977
2.025	1.961	1.948	1.954	Mumme *et al.*, 1995
1.865	1.939	1.926	2.030	Catti *et al.*, 1983

(Fig. 10b) and K(Ca) atoms in *M*(2) site and O vertices of tetrahedron bases are linked into close-packed heterogeneous sheets at levels *x* ~ 1/4 and ~ 3/4 similar to sheets *II* and *III* of glaserite but more corrugated. In the structure of glaserite, difference in heights on axis perpendicular to plane of sheet for neighboring atoms of sheets *II* and *III* are 0.22 Å; in the structure of arkanite, 0.97 Å; and in the structures of α'_H-Ca_2SiO_4 and β-Ca_2SiO_4, 1.10 Å and 1.21 Å, respectively. Deformation of sheets *II* and *III* is also expressed in increasing range of distances between neighboring atoms of the same sheet; in the structure of arkanite, *M*(2) — O distances are within range 2.91 — 3.06 Å, in the structure of α'_H-Ca_2SiO_4, 2.64 — 3.32 Å, and in the structure of monoclinic β modification, 2.37— 3.38 Å. Like the structure of glaserite, sheets *II* and *III* are close-packed and octahedral cavities (the first coordination sphere of 9-fold polyhedra) are occupied by K(Ca) atoms in site *M*(1). Tetrahedral cavities are between O atoms of sheet *II* (or *III*) and O atoms of neighboring bands, with apical vertices of tetrahedra of the same level being opposite oriented. The unit-cell dimension *b* of arkanite and its Ca-Si analogues is determined by O — O distances of sheets *II* and *III* corresponded to edge of tetrahedron and octahedron and approximately is their sum and in perpendicular plane of the CP sheets, dimension a is duplicate heights of identical octahedra around site *M*(1).

As aforementioned, β-modification of Ca_2SiO_4, that is strongly distorted monoclinic analogue of arkanite β-K_2SO_4, is metastable phase. Calculation of local balance of valence forces on anions by techniques suggested in (Brese and O'Keeffe, 1991) for variable models of the β-modification structure (Jost *et al.*, 1977; Mumme *et al.*, 1995; Catti *et al.*, 1983) showed certain excess of negative charge for most anions (Table 4) that in turn is caused by the distance of part of O vertices from centres of *M* polyhedra. The natural calcio-olivine γ-Ca_2SiO_4 has not similar violation of local valence balance. In the examined structure of the mineral, valence forces in anions occupying crystal-chemical sites close to larnite are 2.056, 2.054, and 1.982 [calculated according to (Gobechiya *et al.*, 2008)]. Metastability of β-Ca_2SiO_4 causes the aforementioned significant spread of *M*— O distances in close-packed sheets and high degree of their deformation.

At the transition of β-phase into olivine-type γ-modification, homogeneous sheets (Fig. 10c) consisting of O atoms (at levels on axis *x* ~0.2-0.3 and ~0.7-0.8) similar in atom arrangement to heterogeneous sheets *II* and *III* of the β-Ca_2SiO_4 structure and close-packed are formed in the olivine-type structure. At the transition from β- to γ-modification (see previous part), Ca atoms are displaced to the nearest points with coordinates (0,0,0) and (1/2,0,1/2) from sites *M*(2) of heterogeneous sheets *II* and *III* and O atoms, apical vertices of the β-Ca_2SiO_4 bands arranged at levels on *x* ~0 and ~1/2, respectively, locate in the voided sites. Thus, threes of O atoms, which are bases of Si tetrahedra with apical vertices in neighboring layers, are formed in the homogeneous sheets of γ-Ca_2SiO_4. As above mentioned, sites *M*(1) in the structure of γ-Ca_2SiO_4 are displaced comparatively with corresponding sites in the structure of β-Ca_2SiO_4 and like sites *M*(2), are centres of octahedral cavities whose one half is occupied by Ca atoms. Si atoms center 1/8 of tetrahedral cavities formed between two CP sheets. The unit-cell dimension *b* (6.75 Å) of γ-Ca_2SiO_4 is sum of edge lengths of *M*(1) octahedron (4.18 Å) and Si tetrahedron (2.57 Å), and dimension a is sum of heights of *M*(1) and *M*(2) octahedra (2.79 + 2.28 = 5.07 Å). Increasing dimensions *b* and *c* of γ-Ca_2SiO_4 in comparison with corresponding parameters of the other Ca_2SiO_4 polymorphs is resulted from distortion of

octahedra (elongation along axes *b* and *c*) around Ca in sites *M*(1) and *M*(2) (Fig. 9). Such distortion, in turn, is caused by mismatch of radius (*r*) of $^{[6]}Ca^{2+}$ (*r* = 1.00 Å) and size of octahedral cavity of hexagonal closest packing. This discrepancy is lesser in the structure of olivine-type monticellite $CaMgSiO_4$ (Onken, 1965) (*a* = 4.822, *b* = 6.382, *c* = 11.108 Å, space group *Pcmn*), where octahedral site *M*(2) is occupied by $^{[6]}Mg^{2+}$ (*r* = 0.72 Å) and in the structure of forsterite Mg_2SiO_4 (Fujino *et al.*, 1981) (*a* = 4.753, *b* = 5.978, *c* = 10.190 Å, space group *Pcmn*), dimension *b* being sum of lengths of edge of *M*(2) octahedron (3.384 Å) and edge of tetrahedron (2.594 Å) is comparable with similar dimensions of the other polymorphs of Ca_2SiO_4. Shortening of dimension a of γ-Ca_2SiO_4 in comparison with corresponding parameters (perpendicular to plane of CP sheets) of rhombic and monoclinic polymorphs (Table 1) is due to features of atomic layering: in the structure of γ-Ca_2SiO_4, centres of tetrahedral and octahedral cavities are approximately arranged at the same level on axis a (Fig. 7d) and in the structures of the other modifications, are displaced approximately 1/4 Ta (Fig. 7a, 7b, 7c).

Features of the merwinite and bredigite structures

In geological objects, γ-Ca_2SiO_4 (calcio-olivine), β-Ca_2SiO_4 (larnite) and bredigite, Ca-Mg orthosilicate with formula $Ca_7Mg[SiO_4]_4$ (Moore and Araki, 1976) are extremely rare, whereas merwinite, Ca-Mg orthosilicate with formula $Ca_3Mg[SiO_4]_2$, is more abundant (Moore and Araki, 1973). The structural affinity of these minerals determines similarity of their optical parameters and morphologies. Above-listed minerals are formed under volcanic or subvolcanic conditions characterized by high temperature and low fluid pressure (larnite-merwinite facies by Korzhinsky). Larnite and calcio-olivine can be associated with bredigite, whereas merwinite can be associated with bredigite, rather than larnite or calcio-olivine. Merwinite is more frequently associated with monticellite $CaMgSiO_4$ that is Mg-richer compound in the calcio-olivine Ca_2SiO_4 – forsterite Mg_2SiO_4 series.

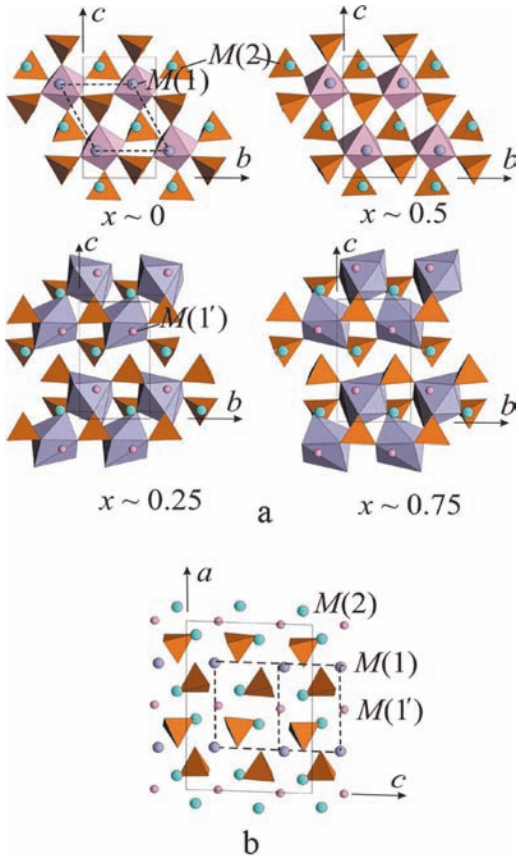

Fig. 11. The structure of merwinite $Ca_3Mg[SiO_4]_2$ projected onto (100) (a) and (010) (b). Mg octahedra with centres in site M(1') (level x ~ 0 and x ~ 0.5) and Ca 8-fold polyhedra with centres in site M(1) (level x ~ 0.25 and x ~ 0.75). Dashed line denotes primary glaserite cell.

In the structure of merwinite $Ca_3Mg[SiO_4]_2$ (Fig. 11a, 11b), Ca atoms occupying sites *M*(1), *M*(2) and Mg atoms in site *M*(1') are arranged like K and Na atoms in the structure of glaserite; the arrangement of Si and O atoms and orientation of tetrahedra around octahedron in rotator are also similar. Distinction of the merwinite structure from the glaserite one is little displacement and turn of Si tetrahedra resulting in the symmetry lowering of merwinite to monoclinic (Table 1) and doubling dimension *a* (Fig. 11c). In the structure of merwinite, atoms form heterogeneous CP sheets composed of Ca and O atoms and analogous to glaserite sheets, while octahedral cavities formed between these sheets are occupied by Mg atoms. The sheets are arranged in pairs at six

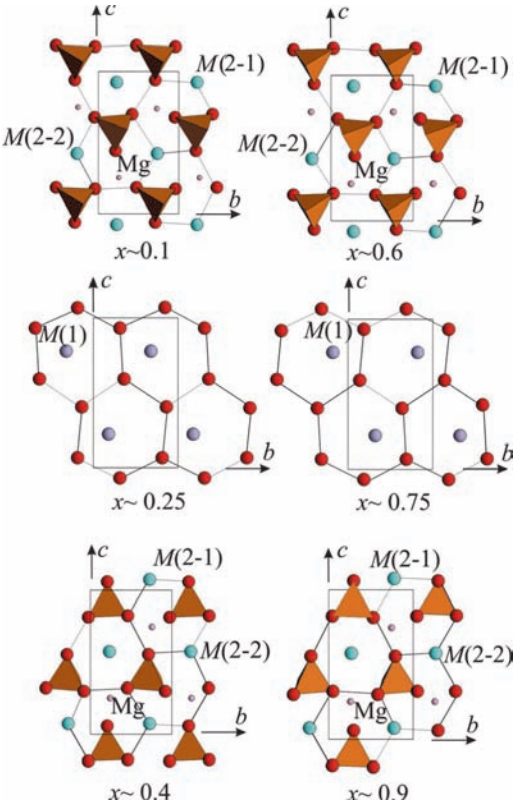

Fig. 12. The close-packed heterogeneous sheets in the structure of merwinite $Ca_3Mg[SiO_4]_2$. Pairs of sheets at levels x ~ 0.1 and x ~ 0.6; x ~ 0.25 and x ~ 0.75; x ~ 0.4 and x ~ 0.9 are bonded by reflection in plane $a_{\perp y}$. Small circles: positions of Mg atoms in the centres of octahedra.

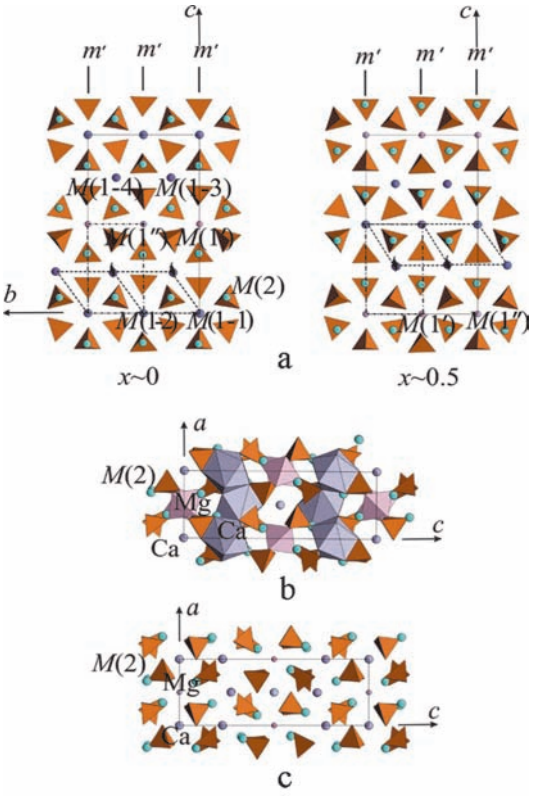

Fig.13. The structure of bredigite $Ca_7Mg[SiO_4]_4$ projected onto: (a) (100); (b, c) (010). In Fig. a, screw axes 2_{1x}, pseudosymmetry elements bonding primary glaserite cells (dashed line) at levels x ~ 0 and x ~ 0.5 and planes of mirror reflection $m_{\perp y}$ linking arkanite cells (dashed-dot line) are shown.

levels on axis x, with each pair being linked through reflection in the *a* plane of glide reflection (Fig. 12). Replacement of Na atoms occupying octahedral cavities (site *M*(1′) in the structure of glaserite) by Mg atoms (with smaller ionic radius) in the structure of mervinite leads to the change of the *M*(1) atom coordination environment. Oxygen atoms at distance of 2.909 Å compose the first coordination (octahedral) sphere around site *M*(1) in the structure of glaserite, whereas in the structure of mervinite, one of such atoms is distant from central atoms for 3.28 Å and the other 3 ligands are out of the radius of 3.5 Å. As a result, zigzag bands consisting of *M*(1) 8-fold polyhedra elongated along axis *b* of the unit cell are formed in the structure of merwinite instead of sheets composed of *M*(1) icosahedra. These bands linked by turn around screw axis 2_{1y} are arranged at two levels along [100] that twice increases the unit-cell parameter of merwinite (a = 13.254 Å) (Table 1) in comparison with corresponding unit-cell dimension of glaserite. At the same time, number of ligands around Ca in site *M*(2) decreases to form 9-fold polyhedra, which are bonded into framework with *M*(1) 8-fold polyhedra.

At the early stages of study of the dicalcium silicate polymorphs, bredigite was identified with α-Ca_2SiO_4 (Bridge, 1966; Tilley and Vincent, 1948) that caused certain confusion. In point of fact, despite similar symmetry and comparability of the unit-cell dimensions of bredigite $Ca_7Mg[SiO_4]_4$ and orthorhombic modifications of Ca_2SiO_4 (Table 1), the structure of the latter is original and is complex combination of structural models of both glaserite and othorhombic arkanite. Part of Ca atoms in sites *M*(1−1) and *M*(1−2) (Fig.

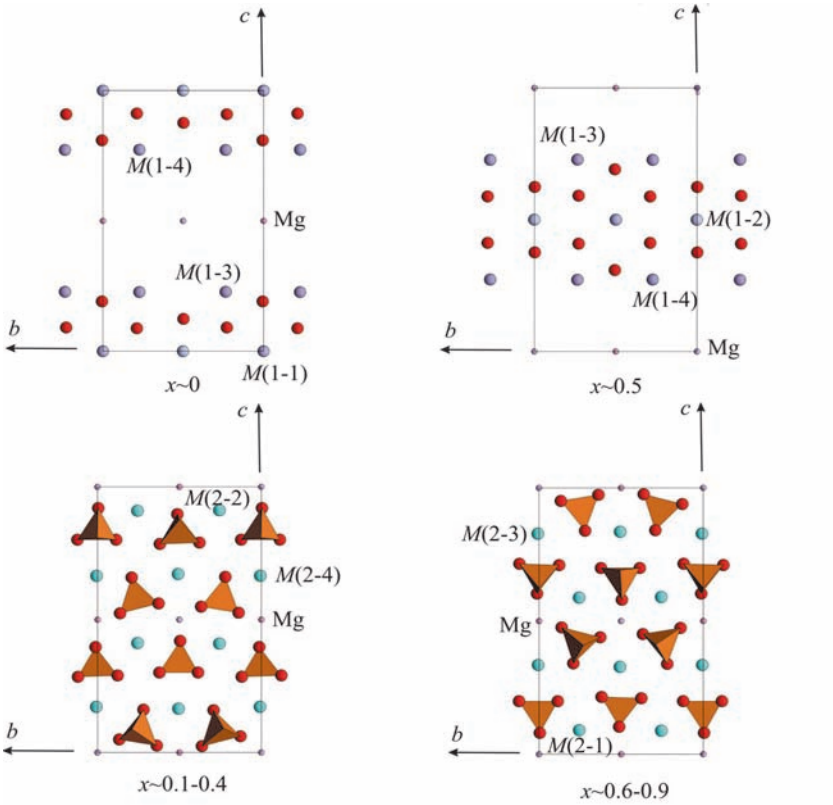

Fig.14. Layering of atoms in the structure of bredigite $Ca_7Mg[SiO_4]_4$: ribbons consisting of Ca atoms in sites M(1) and O atoms (red circles) at levels x ~ 0 and x ~ 0.5 and heterogeneous sheets at levels x ~ 0.1—0.4 and ~ 0.6—0.9. Small circles: positions of Mg atoms in the centres of octahedra.

13a, 13b) are arranged similarly to K atoms in the structure of glaserite, i.e., in the centres of large polyhedra (in this case, 10-ford polyhedra) surrounded by six Si tetrahedra with apical vertices oriented like glaserite. Mg atoms in sites *M*(1′) and *M*(1′′), which are centres of octahedra (Fig. 13c) surrounded by six Si tetrahedra, are arranged at the Ta half both over and below sites *M*(1 − 1) and *M*(1 − 2) like Na in the structure of glaserite. Tetrahedron triplets arranged at two levels on axis *x* are shared for Mg octahedra and *M*(1 − 1) and *M*(1 − 2) 10-fold polyhedra. Another part of Ca atoms in sites *M*(1 − 3) and *M*(1 − 4) centre 9-fold and 8-fold polyhedra surrounded by six Si tetrahedra oriented like in the structures of orthorhombic arkanite β-K_2SO_4, α'_H-Ca_2SiO_4, and α'_L-Ca_2SiO_4; and monoclinic β-Ca_2SiO_4. The residual Ca atoms are arranged both below and over Si tetrahedra in four independent sites *M*(2) in the centres of 10-fold polyhedra close in shape and sizes to corresponding polyhedra of trigonal and orthorhombic polyhedra of Ca_2SiO_4 (Tables 2, 3). Layering of atoms in the structure of bredigite differs from described above. A pair of ribbons consisting of Ca (site *M*(1)) and apical O vertices of Si tetrahedra linked by turn around horizontal 2-fold axes (2_y) are formed at levels ~ 0 and ~ 1/2 on axis *x* (Fig. 14). In addition, Mg atoms in sites *M*(1′) — centres of octahedral cavities formed by O atoms of heterogeneous CP sheets at levels ~ 0.1 − 0.4 and ~ 0.6 − 0.9 on axis *x* — are arranged at the same levels. Like the structures of orthorhombic polymorphs, tetrahedral cavities are formed between O atoms of mentioned sheets and apical O vertices arranged at levels ~ 0 and ~ 0.5 on axis *x*. In this case, tetrahedra belonging to the same sheet-type structures of above described orthorhombic and monoclinic polymorphs of Ca_2SiO_4 have the opposite oriented apical vertices, but alternation of polar tetrahedra in the sheet is different.

Conclusion

Examination of atomic layering in the structures of Ca_2SiO_4 polymorphs indicated

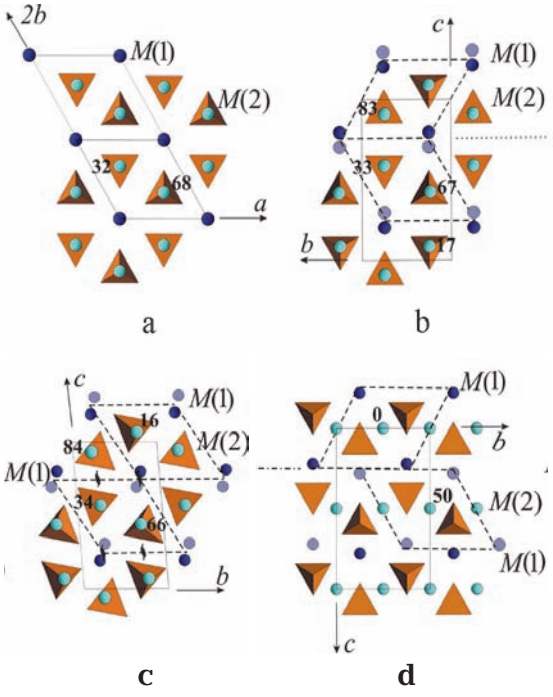

Fig. 15. Idealized projections of the structures: (a) glaserite $K_3Na[SO_4]_2$ and merwinite $Ca_3Mg[SiO_4]_2$; (b) arkanite β-K_2SO_4, α′$_H$-Ca_2SiO_4, and α′$_L$-Ca_2SiO_4; (c) -Ca_2SiO_4; (d) calcio-olivine γ-Ca_2SiO_4. K(Ca) atoms in sites M(1) at levels z(x) ~ 0 (light circles), z(x) ~ 0.5 (dark circles) and in sites M(2) at figured levels on axes z(x). Dashed line: primary glaserite cells bonded through translations (a) and symmetry elements (b – d).

that types of sheets of the aphthitalite (glaserite) structure are realized for merwinite and high-temperature α-modification of Ca_2SiO_4 (model of space group $P\bar{3}m1$) and arkanite β-K_2SO_4, in the structures of high-temperature modifications α′$_H$-Ca_2SiO_4, α′$_L$-Ca_2SiO_4, β-Ca_2SiO_4. Significant spread of distances between Ca and O atoms belonging to the same sheet and neighboring sheets caused by the lesser commensurability (in comparison with K) of their ionic radii necessary to form heterogeneous layers is characteristic of Ca modifications of both layering types. Such structure can be stable only at great thermal vibration of atoms that is probable only at high temperature, therefore pure calcium natural analogues of high-temperature (α, α′$_H$, and α′$_L$) Ca_2SiO_4 modifications can be most probably observable in quenching environment. It provides split atomic sites in their structures; therefore, the model of α modification (space group $P6_3/mmc$) used by Mumme *et al.* (1996) to refine the structure is the most probable. In the structure of α-Ca_2SiO_4 whose symmetry is described by space group $P\bar{3}m1$ the volume of octahedral cavities (distance $M(1') - O = 2.26$ Å) is insufficient for relatively large ($r^{[6]}Ca^{2+} = 1.00$ Å) cation, whereas in the structure of natural merwinite, the similar site is occupied by Mg ($r^{[6]}Mg^{2+} = 0.72$ Å) that operates as stabilizer whose presence provides stable compounds under ambient conditions. Magnesium centering octahedral cavities formed between heterogeneous CP sheets in the structure of bredigite is also stabilizer at the formation of the compound, which is closest in metric characteristics and symmetry to high-temperature α′$_H$-Ca_2SiO_4. The substitution of Mg for Ca in the centres of octahedral cavities in the structures of merwinite and bredigite is accompanied by distortion of heterogeneous CP sheets: differences in heights on axis *x* (Δ*x*) of O atoms forming horizontal bases of tetrahedra are 0.93 Å and 1.15 Å for merwinite and bredigite, respectively. Such deviation causes turn of Si tetrahedra that is also characteristic of transition from α to β modifications of Ca_2SiO_4: for α-Ca_2SiO_4 $\Delta x = 0$; α′$_H$-Ca_2SiO_4 – 0.48Å; β-Ca_2SiO_4 – 0.54 Å.

At the transition from high-temperature to low-temperature polymorphs of aphthitalite (glaserite) and Ca_2SiO_4, number of the nearest ligands around cations *M* and distances cation-anion also decrease (Tables 2, 3). At the same time, decreasing number of shared edges of *M*(1) polyherda and Si tetrahedra on the one hand, and *M*(1) and *M*(2) polyhedra on the other leads to decrease of the density of the structure. In the metastable β-modification of Ca_2SiO_4, that is transitional species between the glaserite and olivine structural types, sizes of *M* polyhedra are the smallest, whereas degree of the CP sheet distortion and turn of SiO_4 tetrahedra are the greatest in comparison with the high-temperature polymorphs of Ca_2SiO_4. In the structure of olivine-type γ-modification of Ca_2SiO_4 and its natural analogue calcio-olivine, anions are hexagonal close-packed, while cations centre octahedral cavities. Aforementioned mismatch of cation radius to size of octahedral cavity at phase transition β $\Rightarrow$ γ results in

strong deformation of Ca polyhedra, which causes frequently observable cracking of the β-Ca_2SiO_4 crystals (larnite) at cooling along with the minimal density and the largest volume of the γ-Ca_2SiO_4 unit cell. This phenomenon is known in technology of silicates as "dusting of larnite".

It is generally known that all aforementioned modifications of Ca_2SiO_4, bredigite, and merwinite are not stable under effect of fluid at decreasing temperature and are broken down to form wide range of calcium hydrosilicates. It is accepted (Taylor, 1996) that this property is predetermined by distortion of their real structures in comparison with initial ideal models. Larnite is also accepted to react with water at temperature slightly below 0°C in contrast to aforesaid minerals. Particularly, it is known that calcio-olivine can intense react with water at > 200°C (Taylor, 1996). Such distinction in behavior of relative minerals appears to be caused by violated local valence balance on anions in the structure of larnite (Table 4). Features of the larnite structure are characterized by extremely rapid (avalanche-like) attack by hydroxyls of the areas with excess negative charge and the structure of larnite is transformed (breaking down) to compensate local charge unbalance. Probably, these factors favor the reaction between larnite and haloids. The water-larnite reaction is practically important. Just high speed of reaction between water and larnite and large volume of newly formed species provide strength of pastematrix in contrast to the other aforementioned calcium silicates.

Taylor (1996) noted that products of phase transformation of Ca_2SiO_4 including olivine-type γ-Ca_2SiO_4, are topotactic formed, i.e., in strict crystallographic orientation with respect to initial matter indicating their structural affinity. Comparative crystal-chemical examination of the structures similar to aphthitalite (glaserite) allowed to reveal for all examined compounds the major structural module, glaserite block $^{[12]}M(1)^{[6]}M(1')^{[10]}M(2)_2[TO_4]_2$ with pseudo-hexagonal symmetry and atom arrangement close to glaserite. The dimensions of transformed glaserite blocks and transition matrix from unit cells of described polymorphs are given in Table 5. Each of above described structures (Fig. 15) is distinguished by the linkage mode of neighboring blocks that causes difference in size in symmetry of unit cells.

Table 5. **Transition matrixes from unit cells of glaserite-type compounds to the unit cell of aphthitalite and dimensions of transformed "glaserite" unit cells**

Compound, formula	Transition matrixes			Dimensions of the "glaserite" unit cell (Å, degree)		
				a	*b*	*c*
				α	β	γ
Arkanite β-K_2SO_4	0	-1	0	5.763	5.820	7.476
	0	0.5	0.5	90	90	119.78
	1	0	0			
α'_H-Ca_2SiO_4	0	-1	0	5.601	5.538	6.871
	0	0.5	0.5	90	90	120.38
	1	0	0			
α'_L-Ca_2SiO_4	0	-1	0	5.590	5.510	6.842
	0	0.5	0.5	90	90	120.48
	0.33	0	0			
Larnite	0	1	0	5.502	5.558	6.745
β-Ca_2SiO_4	0	-0.5	0.5	90	90	123.98
	1	0	0			
Merwinite	0	-1	0	5.293	5.363	6.627
$Ca_3Mg[SiO_4]_2$	0	0.5	-0.5	88.35	90	119.57
	0.5	0	0			
Bredigite	0	-0.5	0	5.455	5.335	6.739
$Ca_7Mg[SiO_4]_4$	0	0.25	0.25	90	90	120.75
	1	0	0			
Calcio-olivine	0	-1	0	6.754	6.544	5.074
γ-Ca_2SiO_4	0	0.5	0.5	90	90	121.07
	1	0	0			

In the structures of glaserite $K_3Na[SO_4]_2$, high-temperature modification α-Ca_2SiO_4 (space group $P\bar{3}m1$), and merwinite $Ca_3Mg[SiO_4]_2$, separated blocks are bonded by translations (Fig. 15a) with the exception of insignificant displacement of atoms in subcells neighboring on axis *a* in case of merwinite (Fig. 11c). Neighboring along [010] and [0 $\bar{1}$1] glaserite blocks, from which the structure of merwinite can be constructed (Fig. 11a, 11b), are linked by translations, while

along [100], by reflection in plane of glide reflection $a_{\perp y}$. Character of combination of the glaserite blocks in the structure of merwinite and close metrics of transformed unit cell (Table 5) and α-Ca_2SiO_4 (Table 1) allow considering merwinite as distorted Ca-Mg silicate analogue of aphthitalite (glaserite) $K_3Na[SO_4]_2$, on the one hand, and as natural distorted Ca-Mg analogue of high-temperature α-modification of Ca_2SiO_4 (its model with space group $P\bar{3}m1$) in whose structure Mg atoms substitutes Ca atoms in site *M*(1′), on the other.

In the structures of orthorhombic arkanite β-K_2SO_4 and its silicate Ca analogues (high-temperature modifications α'_H-Ca_2SiO_4 and α'_L-Ca_2SiO_4), neighboring glaserite blocks (Fig. 15b) are bonded by reflection in plane $a_{\perp z}$ and tripling unit-cell parameter *a* of α'_L-Ca_2SiO_4 is caused by small displacement of atoms in neighboring subcells. In the structure of β-Ca_2SiO_4, neighboring glaserite blocks are linked by rotation around 2-fold screw axis 2_x. The structure of calcio-olivine, γ-Ca_2SiO_4, can be considered as product of the structure of glaserite, where neighboring on axis *c* glaserite-type blocks (Fig. 15d) are linked by the reflection in clinoplane $n_{\perp z}$, i.e., they are displaced to each other for 1/2*Ta* и 1/2*Tb* and in the selected glaserite cell, atoms *M*(1) and Si tetrahedra (without regard for differences in *x* coordinates) are arranged identically to those in the structure of glaserite (Fig. 15a).

The structure of bredigite $Ca_7Mg[SiO_4]_4$ can be also constructed from the glaserite cells (shown in Figs. 13a, 13b as dash lines) under the assumption that atoms of the same variety are arranged in its vertices. The neighboring cells are linked by translations along [100] and [010] and by reflection in clinoplanes $n_{\perp z}$ along [001]. Pairs of blocks arranged at level *z* from 0 to 1/2 are linked with neighboring similar pair along [001] by the rotation around horizontal 2-fold axis 2_y. Furthermore, additional elements of pseudosimmetry bonding neighboring blocks appear in the structure of bredigite (without regard for small displacements of atoms): screw axes $2_1(x)$ parallel to [100] and arranged in points with coordinates *y* and *z* corresponded to sites *M*(1−3) and *M*(1−4); and mirror planes of symmetry $m_{\perp y}$ at levels $y = 0$ and $y = 1/2$ bonding blocks along [010]. The neighboring arkanite blocks, from which the structure of bredigite can be also constructed under the assumption of identical occupation by atoms of points of selected cell and displacement of its top to site *M*(1), can be integrated by the latter operation. Along [001], neighboring arkanite blocks are bonded by axis 2_y. The dimensions of arkanite block (*a*′, *b*′, *c*′) shown in Figs. 13, 13b as chain line are multiple to relevant unit-cell dimensions of bredigite: $a' = a$, $b' = b/2$, $c' = c/2$ (Table 1). In the interior of the blocks, atoms are arranged in the same manner as in the structures of aphthitalite (glaserite) and arkanite, respectively and symmetry lowering and simultaneous increasing unit-cell dimensions of bredigite are determined by the character of layering of selected cells, Mg for Ca substitution, and displacement of atoms.

In all described cases, glaserite blocks are bonded by the symmetry elements of space groups to which arrangement of atoms of the whole structure follows. The additional pseudosymmetry elements also integrate glaserite and arkanite blocks in the structure of bredigite. Topotaxy that is characteristic of the Ca_2SiO_4 polymorphs is caused by close sizes and symmetry of the glaserite blocks (only inversion centres form all symmetry elements are preserved in the selected glaserite cell of each compound) and the same orientation of separated blocks in their structures.

The glaserite modules in the structures of described compounds close in symmetry and composition account for the reversibility of phase transitions between Ca_2SiO_4 polymorphs on the one hand and abundant mineral assemblages of this series on the other. Transition from high-temperature polymorphs α'_H- and α'_L-Ca_2SiO_4 to β-Ca_2SiO_4 can be attributed to deformation without substantial transformation of the structure. Transitions from high-temperature hexagonal α to orthorhombic α'_H modification and from metastable β modification to olivine-type γ-modification are reconstructive when structural type changes. In this case, the structure of γ-Ca_2SiO_4 (calcio-olivine) can

also consists of glaserite-type blocks. Strong drop of density and optical parameters of calcio-olivine in comparison with the other polymorphs emphasizes the structural distinction of this Ca_2SiO_4 modification.

Acknowledgments

We thank N.N. Pertsev for his assistance in examination of paragenetic assemblages of the studied minerals.

References

Barbier J., and Hyde B.G. The structures of the polymorphs of dicalcium silicate, Ca_2SiO_4 // Acta Cryst. B. **1985**. B. 41. P. 383–390.

Bellanca A. Sulla structura dell'aftitalite // Period. Mineral. **1944**. V. 14. P. 67–96.

Brese N.E., and O'Keeffe M. Bond valence parameters for solids // Acta Cryst. B. **1991**. V. 47. P. 192–197.

Bridge, T.E. Bredigite, larnite and dicalcium silicates from Marble Canyon // Amer. Mineral. **1966**. V. 51. P. 1768–1774.

Catti M., Gazzoni G., and Ivaldi G. Structures of twinned β-Sr_2SiO_4 and of γ-$Sr_{1.9}Ba_{0.1}SiO_4$ // Acta Cryst. C. **1983**. C. 39. P. 29–34.

Egorov-Tismenko Yu.K., Sokolova E.V., Smirnova N.L., and Yamnova N.A. Crystal chemical features of minerals similar to the glaserite structural type // Mineral. J. **1984**. V. 6 (6). P. 3–9. (In Russian.)

Eysel W. and Hahn T. Polymorphism and solid solution of Ca_2GeO_4 and Ca_2SiO_4 // Z. Kristallogr. **1970**. V. 131. P. 322–341.

Fujino K., Sasaki S., Takäuchi Y., and Sadanaga R. X-ray determination of electron distributions in forsterite, fayalite and tephroite // Acta Cryst. B. **1981**. B. 37. P. 513–518.

Gobechiya E.R., Yamnova N.A., Zadov A.E., and Gazeev V.M. Calcio-olivine, γ-Ca_2SiO_4: I. Rietveld refinement of the crystal structure // Crystallogr. Rep. **2008**. V. 53 (3). P. 359–364. (In Russian.)

Il'inets A.M. and Bikbau M.Ya. Structural mechanism of polymorphous transitions of dicalcium silicate, Ca_2SiO_4: I. Atomic structure of polymorphous modifications // Crystallographia. **1990**. V. 35 (1). P. 84–90. (In Russian.)

Jost K.H., Ziemer B., and Seydel R. Redetermination of the structure of β-dicalcium silicate // Acta Cryst. B. **1977**. B. 33. P. 1696–1700.

McGinnety J.A. Redetermination of the structures of potassium sulphate and potassium chromate: the effect of electrostatic crystal forces upon observed bond lengths // Acta Cryst. B. **1972**. B. 28. P. 2845–2852.

Midgley C.M. The crystal structure of dicalcium silicate // Acta Cryst. **1952**. V. 5. P. 307–312.

Miyake M., Morikawa H., and Iwai S.I. Structure reinvestigation of the high-temperature form of K_2SO_4 // Acta Cryst. B. 1980. B. 36. P. 532–536.

Moore P.B. Bracelets and Pinwheels: A topological-geometrical approach to the calcium orthosilicate and alkali sulfate structures // Amer. Mineral. **1973**. V. 58. P. 32–42.

Moore P.B. The glaserite, $K_3Na[SO_4]_2$, structure type as a "super" dense-packed oxide: evidence for icosahedral geometry and cation-anion mixed layer packings // Neues Jahrb. Mineral. Abhandlungen. 1976. Bd. 127. No 2. P. 187–196.

Moore P.B. Complex crystal structures related to glaserite, $K_3Na[SO_4]_2$: evidence for very dense packings among oxysalts // Bull. Mineral. **1981**. V. 104 (4). P. 536–547.

Moore P.B. and Araki T. Atomic arrangement of merwinite, $Ca_3Mg[SiO_4]_2$, an unusual dense-packed structure of geophysical interest // Amer. Mineral. **1973**. V. 57. P. 1355–1374.

Moore P.B. and Araki T. The crystal structure of bredigite and the genealogy of some alkaline earth orthosilicates // Amer. Mineral. **1976**. 61. P. 74–87.

Mumme W.G., Cranswick L., and Chakoumakos B. Rietveld crystal structure refinements from high temperature neutron powder diffraction data for the polymorphs of dicalcium silicate // Neues Jahrb. Mineral. Abhandlungen. **1996**. Bd. 170 (2). P. 171–188.

Mumme W.G., Hill R.J., Bushnell G.W., and Segnit E.R. Rietveld crystal structure refinements, crystal chemistry and calculated powder diffraction data for the polymorphs of dicalcium silicate and related phases // Neues Jahrb. Mineral. Abhandlungen. **1995**. Bd. 169 (1). P. 35–68.

Okada K. and Ossaka J. Structures of potassium sodium sulphate and tripotassium sodium disulphate // Acta Cryst. B. **1980**. B. 36. P. 919–921.

Onken H. Verfeinerung der Kristallostructur von Monticellit // Tschermaks Mineralogische und Petrographische Mitteilungen. **1965**. No 10. S. 34–44. (In German.)

Taylor H.F.W. Cement chemistry. T. Telford, London. **1996**. 560 p.

Tilley C.E., Vincent H.C.G. The occurrence of an orthorhombic high temperature form of Ca_2SiO_4 (bredigite) in Scawt Hill contact zone and as a constituent of slabs // Mineral. Mag. **1948**. V. 28. P. 255–271.

Zadov A.E., Gazeev V.M., Pertsev N.N., Gurbanov A.G., Yamnova N.A., Gobechiya E.R., and Chukanov N.V. Discovery and investigation of a natural analog of calcio-olivine (γ-Ca_2SiO_4) // Dokl. Earth Sci. **2008**. V. 423A (9). P. 1431–1434. (In Russian.)